Materials Science and Engineering A 528 (2011) 6838–6843

Contents lists available at ScienceDirect

Materials Science and Engineering A

journal homepage: www.elsevier.com/locate/msea

Dynamic compressive constitutive relation and shearing instability of metallic neodymium

Wang Huanran, Cai Canyuan, Chen Danian*, Ma Dongfang, Hou Yanjun, Wu Shanxing

Mechanics and Materials Science Research Center, Ningbo University, Zhejiang 315211, China

ARTICLE INFO

Article history:
Received 22 February 2011
Received in revised form 3 May 2011
Accepted 26 May 2011
Available online 21 June 2011

Keywords:
Metallic Nd
Dynamic compression
Constitutive relation
Large deformation
Shearing instability

ABSTRACT

Based on static tests on MTS and dynamic tests on split Hopkinson pressure bar (SHPB) during the first loading, this study determined the dynamic compressive constitutive relation of metallic Nd. Based on large deformations of metallic Nd specimens generated by the multi-compressive loadings during SHPB tests, and recorded by a high-speed camera, the results of numerical simulations for SHPB test processes were used to extend the determined constitutive relation from small strain to large strain. The shearing instability strain in dynamic compressive deformations of metallic Nd was estimated with the extended constitutive relation according to the criterion given by Batra and Wei, and was compared with the average strain of recovered specimens.

1. Introduction

Rare earth (RE) elements can be used across all areas, in traditional industries such as metallurgy, machinery, chemicals, textile and agriculture. RE new products have emerged and led to the formation of a group of new industries. The characterizations of dynamic constitutive behavior of RE elements are very important for their potential engineering applications. However, no data is currently available on dynamic constitutive behavior for RE elements.

Whenever a material made of two or more component phases with different properties is subjected to stress, in general, the phases deform differently. This results in additional interactive stresses and strains and their magnitude depends on such factors as the property difference between phases and morphology and volume fraction of phases. It was reviewed by Ankem et al. [1] to describe how the various parameters such as morphology and volume percent of phases affect the mechanical properties of two-phase materials. It can be expected that the dynamic constitutive behavior for RE elements will be used to design and select multi-phase materials containing RE for various engineering applications.

Strain rate dependent compressive deformation behavior of Nd-based bulk metallic glass was characterized by Liu et al. [2] over a wide strain rate range at room temperature. The impact stability of sintered Nd–Fe–B magnets has been investigated by Wang et al. [3] by using a falling-weight impact test. Equation of state and phase transformations for Nd at ultra-high pressures were studied by Akella et al. [4]. In this paper, the compressive behavior of metallic Nd over a wide range of strain rates at different temperatures was investigated, both static tests on MTS and dynamic tests on split Hopkinson pressure bar (SHPB) were carried out. The empirical constitutive relation was determined for metallic Nd in the first loading duration of SHPB tests. The determined constitutive relation of metallic Nd was checked by using the numerical simulations of SHPB tests in the first loading duration. The reflected and transmitted pulses of SHPB tests computed with the determined constitutive relation for metallic Nd specimen can be consistent with the experimental data to a certain extent. The constitutive relation determined in a certain range of strains was employed and adjusted in numerically simulating large deformations of metallic Nd specimens generated by multi-compression in SHPB tests and recorded by a high-speed camera. The result of 3D Supper Depth Digital Microscope (SDDM) investigation of the recovered metallic Nd specimen was also shown to indicate the shearing instability of the specimen. The shearing instability strain in dynamic compressive deformations of metallic Nd was estimated with the adjusted constitutive relation according to the criterion given by Batra and Wei [5], and was compared with the average strain of recovered specimens.

2. Experimental determination of dynamic compressive constitutive relation of metallic Nd

Cylindrical specimens 6 mm in diameter and 4 mm in length were prepared from metallic Nd ingots with a purity of 99.0%. The

* Corresponding author. Tel.: +86 574 87600981; fax: +86 574 87608358.
E-mail address: chdnch@nbu.edu.cn (C. Danian).

0921-5093/$ – see front matter © 2011 Elsevier B.V. All rights reserved.
doi:10.1016/j.msea.2011.05.066

Table 1
Chemical compositions (wt%) of the studied metallic Nd.

Nd ≥ 99.0	Sm ≤ 0.005	Y ≤ 0.01	Dy ≤ 0.05	Tm ≤ 0.05	Eu ≤ 0.05	Tb ≤ 0.05	Ho ≤ 0.05	Gd ≤ 0.05	Fe ≤ 0.5	C ≤ 0.05	Cu ≤ 0.05
Mg ≤ 0.05	Al ≤ 0.15	Ca ≤ 0.05	Ti ≤ 0.05	Si ≤ 0.05	Mn ≤ 0.05	Mo ≤ 0.05	W ≤ 0.05	Cr ≤ 0.05	Ni ≤ 0.05	N ≤ 0.05	O ≤ 0.05

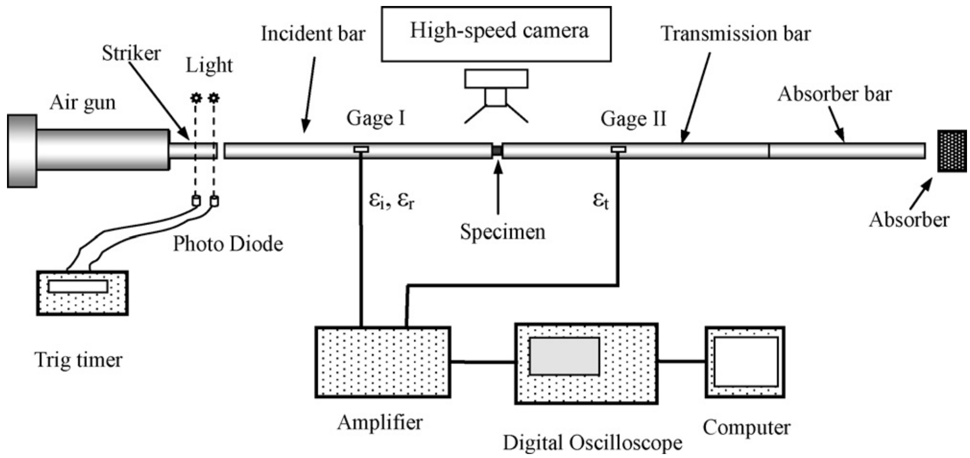

Fig. 1. A split Hopkinson pressure bar test.

chemical compositions (wt%) of studied metallic Nd are given in Table 1. The quasi-static compression tests were carried out on MTS, whereas the dynamic compression tests were performed on SHPB shown in Fig. 1. A high strength steel was used for the striker, incident bar and transmitter bar 14.5 mm in diameter. As the incident bar was struck, a compressive wave was generated and propagated through the incident bar. At the interface between the incident bar and the specimen, a part of the compressive wave reflected back to the incident bar and the remaining energy transmitted into the specimen and transmitter bar. The geometry of SHPB specimens was required to reduce ring-up time, inertial effects, and to result in uniaxial stress and uniform stress and strain states in specimens during the first loading in SHPB tests. Using one-dimensional elastic wave theory, the stress $\sigma(t)$, strain $\varepsilon(t)$ and strain rate $\dot{\varepsilon}(t)$ of the specimen under uniform stress and strain states can be calculated.

$$\sigma(t) = \frac{A_0}{A_s} E_0 \varepsilon_t(t) \tag{1}$$

$$\varepsilon(t) = -\frac{2C_0}{L_s} \int_0^t \varepsilon_r(t) \mathrm{d}t \tag{2}$$

$$\dot{\varepsilon}(t) = -\frac{2C_0}{L_s} \varepsilon_r(t) \tag{3}$$

where t is the time, $\varepsilon_t(t)$ and $\varepsilon_r(t)$ are the strain signals of the transmitted wave and reflected wave, respectively. E_0 and A_0 are the elastic modulus, cross-sectional area of the incident bar and transmitted bar, respectively. C_0 is the transmitting speed of elastic stress wave in bars, L_s and A_s are the length and cross-sectional area of testing part of the specimen.

The experimental results of metallic Nd in quasi-static compression tests on MTS and in dynamic compression tests on the SHPB at different strain rates and temperatures are shown in Figs. 2 and 3, respectively. At low (quasi-static) strain rate, metallic Nd is known to work harden along the well-known relationship.

$$\sigma = \sigma_0 + B\varepsilon^n \tag{4}$$

where σ_0 is the yield stress, n is the work-hardening coefficient, and B is the preexponential factor. The effects of strain rate and temperature are separately given in Fig. 3(a) and (b). The effect of temperature on the flow stress can be represented by

$$\sigma = \sigma_r \left[1 - \left(\frac{T - T_r}{T_m - T_r} \right)^m \right] \tag{5}$$

where T_m is the melting point, T_r is a reference temperature at which σ_r, a reference stress, is measured, and T is the temperature for which σ is calculated. The effect of strain rate, which is intimately connected with the evolution of the microstructures, can be simply expressed by

$$\sigma \propto \ln\dot{\varepsilon} \tag{6}$$

This relationship is observed at strain rates that are not too high.

The experimental results of metallic Nd were fitted by Johnson–Cook (J–C) [6] type constitutive relation.

$$\sigma = f(\varepsilon,\ \dot{\varepsilon},\ T) = \left(\sigma_0 + B\varepsilon^n\right) \left(1 + C \ln \frac{\dot{\varepsilon}}{\dot{\varepsilon}_0}\right) \left[1 - (T^*)^m\right] \tag{7}$$

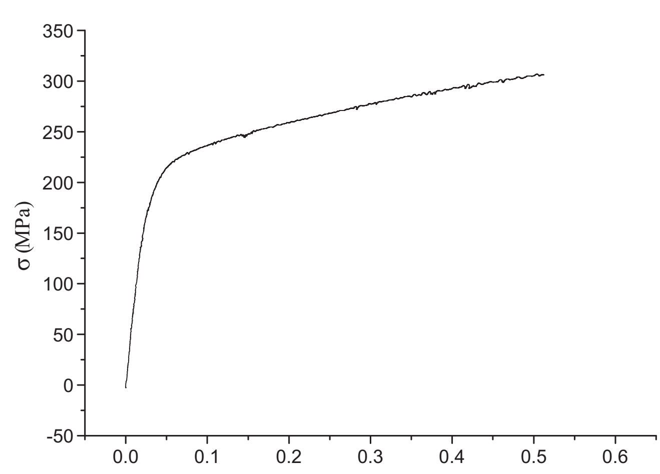

Fig. 2. Stress–strain of metallic Nd under quasi-static compression.

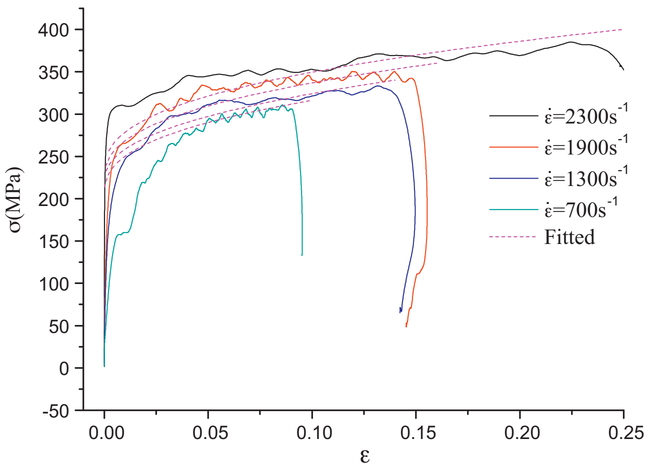

(a) At different strain rates and normal temperature

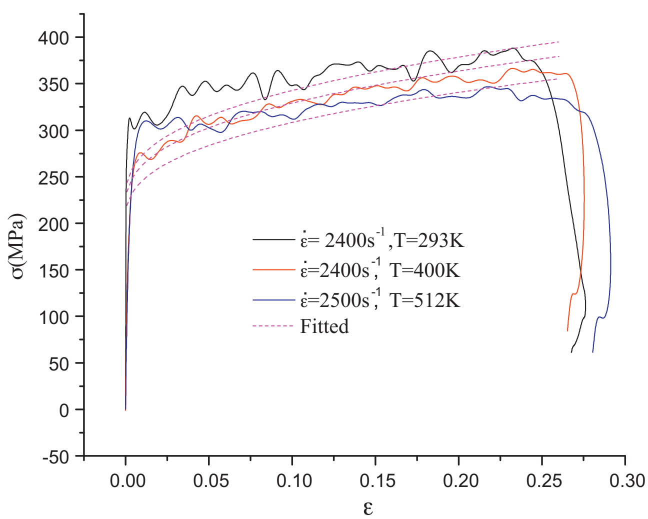

(b) At a certain strain rate and different temperatures

Fig. 3. Stress–strain of metallic Nd under dynamic compression at different strain rates and temperatures. (a) At different strain rates and normal temperature. (b) At a certain strain rate and different temperatures.

where

$$T^* = \frac{T - T_r}{T_m - T_r} \tag{8}$$

$\sigma_0 = 154$ MPa, $B = 197$ MPa, $n = 0.38$, $C = 0.058$, $m = 1.42$. The determination of parameters in the constitutive relation was based primarily on direct correlation of the influence of the parameters in the equations with particular response characteristics. The stress–strain curves of metallic Nd fitted with J–C constitutive relation are compared with experimental data in Fig. 3.

It was indicated by Meyers [7] that since there is a variety of deformation substructures, dependent on strain rate, temperature and stress state, one has to add the general term "deformation history" to the equation above:

$$\sigma = f(\varepsilon,\ \dot{\varepsilon},\ T,\ \text{deformation history}) \tag{9}$$

Here, the constitutive relation is given by reducing the stress and strain (second-order tensor) to effective stress σ and strain ε (scalar quantities).

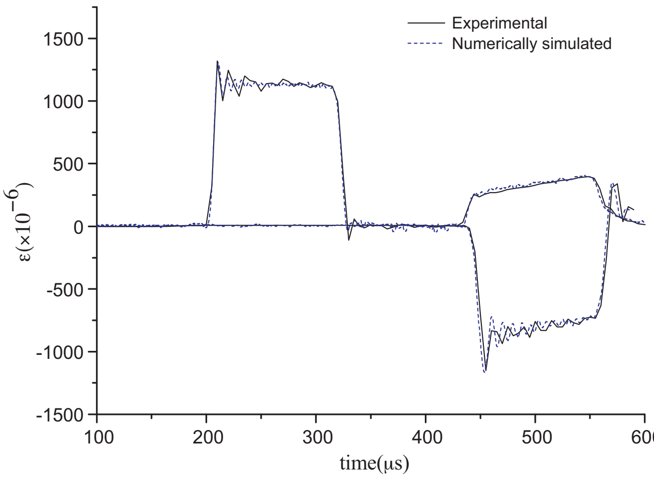

Fig. 4. Comparison between numerically simulated and experimental data for a SHPB test at $\dot{\varepsilon} = 2400\ \mathrm{s}^{-1}$, $T = 293$ K.

3. Checking of the determined constitutive relation of metallic Nd

It should be noted that strain rates $\dot{\varepsilon}$ indicated in Fig. 3 are average value whereas strain rates in the specimen during SHPB tests are in wide range. Furthermore, stresses and strains in the specimen are only just uniform in a certain time interval and the stresses in the specimen are approximately uniaxial even in the first loading duration of SHPB tests. Therefore, the determined constitutive relation of metallic Nd should be checked by using the numerical simulations of SHPB tests. The numerical simulations of SHPB tests were performed by using LS-DYNA [8]. The stresses σ_{ij} are expressed as follows in LS-DYNA [8]:

$$\sigma_{ij} = -(p + q) + S_{ij} \tag{10}$$

where p, q, and S_{ij} are pressure, artificial viscosity and deviatoric stresses, respectively. Up to the Hugoniot elastic limit, p is given by $k\ln(\rho_0/\rho)$, where k, ρ_0, ρ are bulk modulus, initial density and instantaneous density, respectively. For stresses above the Hugoniot elastic limit, the Gruneisen equation of state is adopted, and p is given by

$$p = \frac{\rho_0 C_1^2 \mu[1 + (1 - (\Gamma_0/2))\mu]}{[1 - (S_1 - 1)\mu]^2} + \Gamma_0 U \tag{11}$$

where $\mu = \rho/\rho_0 - 1$, Γ_0 and U are the Gruneisen parameter and specific energy, respectively. C_1 and S_1 are material constants. For metallic Nd, $C_1 = 2.08$ Km/s [9], $S_1 = 1.015$ [9], $\Gamma_0 = 0.82$ [10]. Deviatoric stresses S_{ij} are computed by Hooke's law and dynamic constitutive relation. The determined constitutive relation Eq. (7) was used in numerical simulations. The reflected and transmitted pulses computed with the determined constitutive relation for metallic Nd specimens can be consistent with the experimental data to a certain extent as shown in Figs. 4 and 5.

It is clear that the stress reducing with increasing deformation in Fig. 3 was due to the first loading duration in SHPB tests. In fact, specimens are subjected to multi-compression rather than a single compression, on account of the interactions of compression waves with contact discontinuities. The typical velocity V of the interface between the specimen and the incident bar, generated by the striker bar at velocity of 11.6 m/s in the SHPB shown in Fig. 2, was numerically simulated by using LS-DYNA [8] and was shown in Fig. 6. Large deformations of specimens generated by multi-compression were recorded by a high-speed camera as shown in Fig. 7, the time-interval between each image being 20 μs. Since there is a variety of deformation substructures in multi-

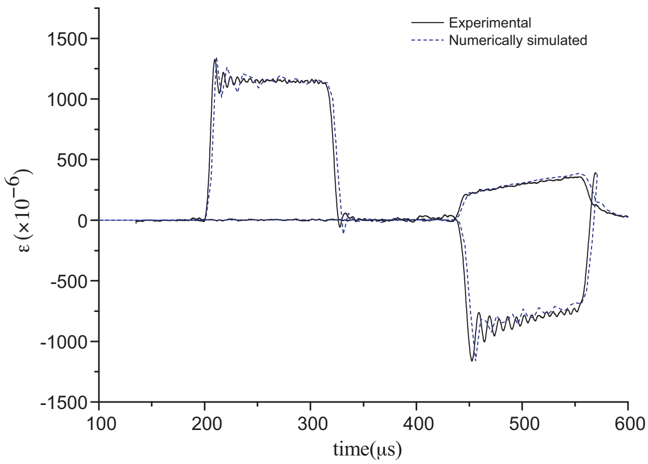

Fig. 5. Comparison between numerically simulated and experimental data for a SHPB test at $\dot{\varepsilon} = 2400\ \mathrm{s}^{-1}$, $T = 400$ K.

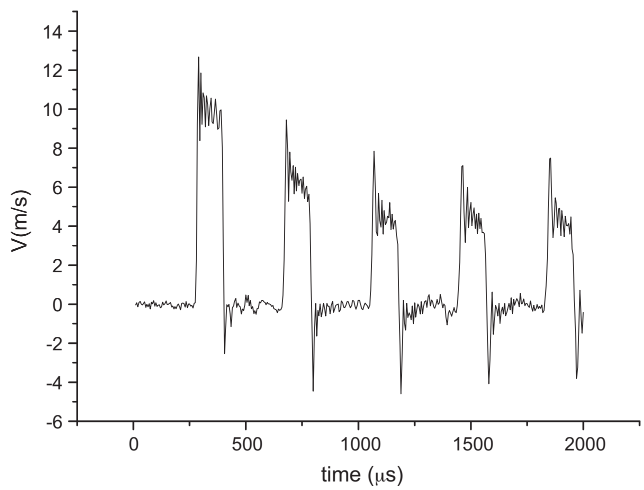

Fig. 6. Computed velocity history of the interface between the incident bar and the specimen generated by the striker at velocity of 11.6 m/s ($\dot{\varepsilon} = 2400\ \mathrm{s}^{-1}$, $T = 293$ K).

compression, dependent on strain, strain rate and temperature, the dependence of the constitutive relation of metallic Nd on deformation history should be investigated. The constitutive relation determined in the first loading duration of SHPB tests was employed and adjusted in numerically simulating large deformations of specimens recorded by the high-speed camera. For large deformations of specimens, the adopted method for determination of the adjusted parameters in the constitutive relation involves assuming an original value for a parameter, comparing computed and experimental large deformations of specimens, and then refining the values by an iteration procedure. The adjusted constitutive relation of metallic Nd is as follows:

$$\sigma = \begin{cases} (154 + 197\varepsilon^{0.38})(1 + 0.058 \ln \dot{\varepsilon})[1 - (T^*)^{1.42}], & \varepsilon \le 0.3 \\ (154 + 197\varepsilon^{0.48})(1 + 0.058 \ln \dot{\varepsilon})[1 - (T^*)^{1.42}], & \varepsilon > 0.3 \end{cases} \quad (12)$$

which indicates that the work-hardening coefficient is the main base.

The deformations of specimens computed with original and adjusted constitutive relations are compared with experimental results in Fig. 8 for the SHPB test at $\dot{\varepsilon} = 2400\,\mathrm{s}^{-1}$, $T = 298$ K.

4. Shearing instability strain in dynamic compressive deformation of metallic Nd

The recovered metallic Nd specimen for the SHPB test at $\dot{\varepsilon} = 2500\,\mathrm{s}^{-1}$, $T = 512$ K shows signs of shearing fracture in Fig. 9, the average strain of which is 0.624. The result of SDDM investigation of the recovered metallic Nd specimen is shown in Fig. 10.

Recently, Batra and Wei [5] analyzed the stability of homogeneous simple tensile/compressive deformations of an isotropic heat-conducting thermoviscoplastic bar by studying the growth of infinitesimal perturbations superimposed upon a homogeneous deformation. For locally adiabatic deformations, the following instability criterion was given:

$$\beta\sigma^0 P_0 - \rho C^*(Y_0 f^0 - \sigma^0) = \rho C^* Q_0 \quad (13)$$

where

$$P_0 = -\frac{\partial\sigma}{\partial T}\Big|_{S=S^0} \quad (14)$$

$$Q_0 = \frac{\partial\sigma}{\partial\varepsilon}\Big|_{S=S^0} \quad (15)$$

$$Y_0 = \frac{\partial\sigma}{\partial\phi}\Big|_{S=S^0} \quad (16)$$

$$f^0 = \frac{\partial\phi}{\partial\varepsilon}\Big|_{S=S^0} \quad (17)$$

$$S^0(t) \equiv (\varepsilon^0(t),\ \sigma^0(t),\ T^0(t),\ \phi^0(t)) \quad (18)$$

ϕ is associated with dissipative mechanisms, C^* and β are the specific heat and the Taylor–Quinney factor describing the fraction of plastic working converted into heating. $S^0(t)$ is corresponding to homogeneous deformations of the bar. In the absence of internal variables (i.e. $Y_0 = 0$), the instability criterion Eq. (13) differs from that $(\beta\sigma^0 P_0/(\rho C^* Q_0) = 1)$ in the simple shearing deformations due

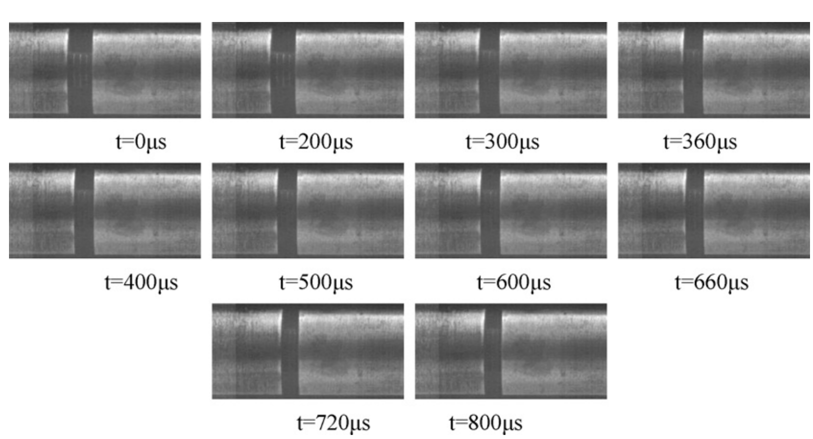

Fig. 7. The high-speed camera image of the deformations of the metallic Nd specimen generated by the striker at impact velocity of 11.6 m/s ($\dot{\varepsilon} = 2400\ \mathrm{s}^{-1}$, $T = 293$ K).

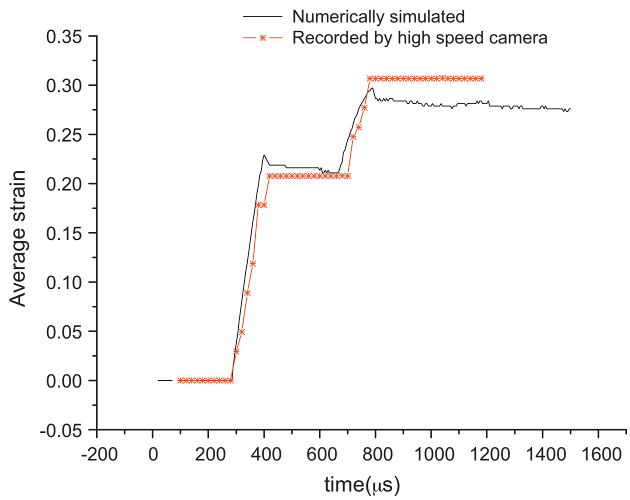

(a) Computed with the original constitutive relation

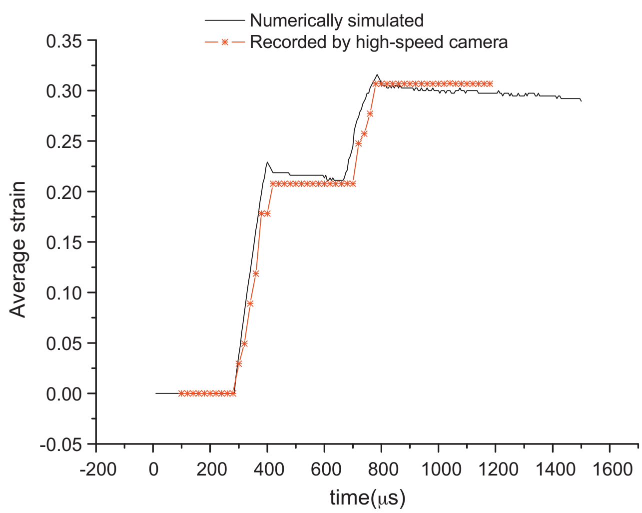

(b) Computed with the adjusted constitutive relation

Fig. 8. Comparison between the numerically computed and experimentally recorded average strains of the metallic Nd specimen for the SHPB test at $\dot{\varepsilon} = 2400\ \mathrm{s}^{-1}$, $T = 293$ K. (a) Computed with the original constitutive relation. (b) Computed with the adjusted constitutive relation.

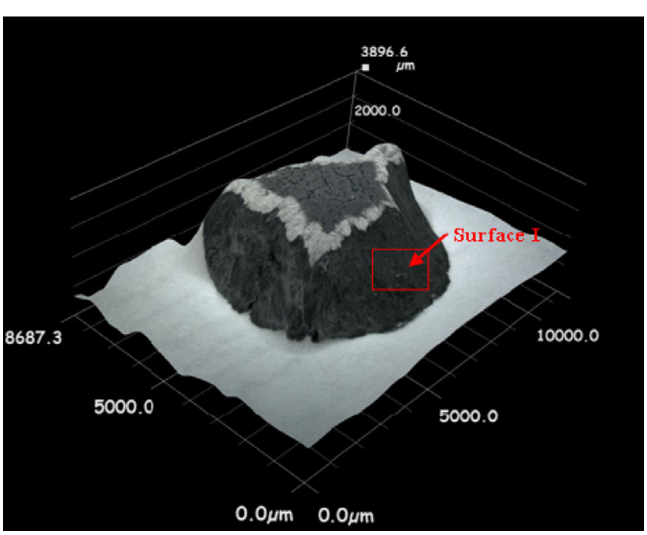

Fig. 9. The recovered metallic Nd specimen for the SHPB test at $\dot{\varepsilon} = 2500\,\mathrm{s}^{-1}$, $T = 512$ K.

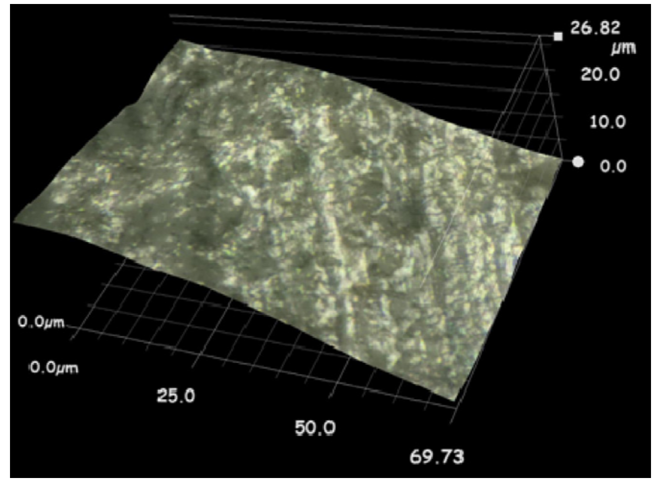

Fig. 10. The results of SDDM investigation on surface I of the recovered metallic Nd specimen for the SHPB test at $\dot{\varepsilon} = 2500\,\mathrm{s}^{-1}$, $T = 512$ K.

to the change in the area of cross-section. The instability strain ε_C of shearing deformation can be estimated with

$$\frac{\beta}{T_m - T_r}(\sigma_0 + B\varepsilon_C^n)^2 \left(1 + C \ln \frac{\dot{\varepsilon}_C}{\dot{\varepsilon}_0}\right) m(T^*)^{m-1} = B\rho C^* n\varepsilon_C^{n-1} \tag{19}$$

for constitutive relation Eqs. (7) and (8). The shearing instability strain ε_C of metallic Nd for the SHPB test at $\dot{\varepsilon} = 2500\,\mathrm{s}^{-1}$ and $T = 512$ K, estimated from Eq. (19) is 0.634, which is close to the experimental result of 0.624.

5. Conclusions

(1) Both compressive tests, static on MTS and dynamic on SHPB, were carried out for metallic Nd. The effects of strain rate and temperature were separately given. The effect of strain rate connected with the evolution of the microstructure and the effect of temperature involved with melting point were represented by empirical relations. A J–C type constitutive relation of metallic Nd was determined by using the first loading of SHPB tests.
(2) The determined constitutive relation of metallic Nd was checked by using the numerical simulations of SHPB tests in the first loading duration. The reflected and transmitted pulses of SHPB tests computed with the determined constitutive relation for metallic Nd specimen can be consistent with the experimental data to a certain extent.
(3) The multi-compressive loadings in SHPB tests for metallic Nd specimens, which were recorded by a high-speed camera, were used to investigate large deformations of specimens and the dependence of the constitutive relation of metallic Nd on deformation history intimately connected with a variety of deformation substructures.
(4) The constitutive relation of metallic Nd determined in small strain was adjusted in numerically simulating large deformations of metallic Nd specimens recorded by the high-speed camera. The adjusted constitutive relation revealed the multi-compressive behavior of metallic Nd, which indicated that the work-harding coefficient was the main base.
(5) The results of SDDM investigation of the recovered metallic Nd specimen showed the shearing fracture. The shearing instability strain in dynamic compressive deformation of metallic Nd was estimated with the adjusted constitutive relation according to the criterion given by Batra and Wei [5], and was compared with the average strain of recovered specimens.

Acknowledgement

The authors acknowledge the financial support from the National Nature Science Foundation of China under grant no. 10872100 and no. 11072118.

References

[1] S. Ankem, H. Margolin, C.A. Greene, B.W. Neuberger, P.G. Oberson, Prog. Mater. Sci. 51 (2006) 632–709.
[2] L.F. Liu, L.H. Dai, Y.L. Bai, B.C. Wei, G.S. Yu, Intermetallics 13 (2005) 827–832.
[3] H.J. Wang, A.H. Li, M.G. Zhu, W. Li, J. Magn. Magn. Mater. 307 (2006) 268–272.
[4] J. Akella, G.S. Smith, J.Z. Hu, S. Weir, Equation of state and phase transformations study of Nd at ultra-high pressures, UCRL-JC-108610, 1991, in: Proceedings of the XIII AIRAPT Conference, Bangalore, India, October 7–11, 1991.
[5] R.C. Batra, Z.G. Wei, Int. J. Impact Eng. 34 (2007) 448–463.
[6] G.R. Johnson, W.H. Cook, Proceedings of Seventh International Symposium on Ballistics, The Hague, The Netherlands, 1983, pp. 541–547.
[7] M.A. Meyers, Dynamic Behavior of Materials, John Wiley & Sons, Inc., Newyork, Chichester, Brisbane, Toronto, Singapore, 1994, pp. 323–325.
[8] J.O. Hallquist, LS-DYNA Keywords Use's Manual (Version 970), LSTC, USA, 2003, April.
[9] S.P. Marsh, LASL Shock Hugoniot Data, University of California Press, Los Angels, London & Berkely, 1980.
[10] K.A. Gschneidner, in: F. Seitz, D. Turnbull (Eds.), Solid State Physics, 16, Academic Press, New York & London, 1965, pp. 275–426.